land

MDPI

Review

Advancements in Forest Monitoring: Applications and Perspectives of Airborne Laser Scanning and Complementarity with Satellite Optical Data

Costanza Borghi [1,2], Saverio Francini [3,*], Giovanni D'Amico [1], Ruben Valbuena [4] and Gherardo Chirici [1,2]

[1] Department of Agriculture, Food, Environment and Forest Science and Technology (DAGRI), University of Florence, 500145 Florence, Italy; costanza.borghi@unifi.it (C.B.); giovanni.damico@unifi.it (G.D.); gherardo.chirici@unifi.it (G.C.)
[2] Fondazione per il Futuro delle Città, 50121 Firenze, Italy
[3] Department of Science and Technology of Agriculture and Environment (DISTAL), University of Bologna, 40126 Bologna, Italy
[4] Department of Forest Resource Management, Swedish University of Agricultural Sciences, 90183 Umea, Sweden; ruben.valbuena@slu.se
* Correspondence: saverio.francini@unibo.it

Abstract: This study reviews research from 2010 to 2023 on the integration of airborne laser scanning (ALS) metrics with satellite and ground-based data for forest monitoring, highlighting the potential of the combined use of ALS and optical remote sensing data in improving the accuracy and the frequency. Following an in-depth screening process, 42 peer-reviewed scientific manuscripts were selected and comprehensively analyzed, identifying how the integration among different sources of information facilitate frequent, large-scale updates, crucial for monitoring forest ecosystems dynamics and changes, aiding in supporting sustainable management and climate smart forestry. The results showed how ALS metrics—especially those related to height and intensity—improved estimates precision of forest volume, biomass, biodiversity, and structural attributes, even in dense vegetation, with an R^2 up to 0.97. Furthermore, ALS data were particularly effective for monitoring urban forest variables (R^2 0.83–0.92), and for species classification (overall accuracy up to 95%), especially when integrated with multispectral and hyperspectral imagery. However, our review also identified existing challenges in predicting biodiversity variables, highlighting the need for continued methodological improvements. Importantly, while some studies revealed great potential, novel applications aiming at improving ALS-derived information in spatial and temporal coverage through the integration of optical satellite data were still very few, revealing a critical research gap. Finally, the ALS studies' distribution was extremely biased. Further research is needed to fully explore its potential for global forest monitoring, particularly in regions like the tropics, where its impact could be significant for ecosystem management and conservation.

Keywords: airborne laser scanner; biodiversity; remote sensing; sustainable forest management

Academic Editors: Heiko Balzter and Dietrich Schmidt-Vogt

Received: 21 January 2025
Revised: 6 February 2025
Accepted: 5 March 2025
Published: 8 March 2025

Citation: Borghi, C.; Francini, S.; D'Amico, G.; Valbuena, R.; Chirici, G. Advancements in Forest Monitoring: Applications and Perspectives of Airborne Laser Scanning and Complementarity with Satellite Optical Data. *Land* **2025**, *14*, 567. https://doi.org/10.3390/land14030567

1. Introduction

Forests cover one-third of the Earth's land surface, absorb significant anthropogenic carbon emissions, and play a critical role in mitigating climate change [1]. Along with their contribution to the carbon cycle [2], the ecosystem services provided by forests encompass a full spectrum of provisioning [3,4], regulating [5], and cultural [6] services. However,

forests are vulnerable to climate change impacts, especially due to the recent intensification in disturbance regimes [7]. Thus, the demand for spatially explicit, up-to-date, and reliable forest data has been growing over recent decades, in order to fulfill the need for regional and global monitoring systems aimed at tracking changes—both due to natural and anthropogenic activities—in forest ecosystems [8,9]. At the national level, National Forest Inventories (NFIs) represent the official source of forest statistics [10], mostly relying on in situ data [11,12]. Despite their significant role in forest assessment, ground-based data alone presents several drawbacks in large-scale forest ecosystem monitoring due to their high operational costs (both in terms of time and money), the need for standardization and harmonization [13], infrequent and scattered updates [14], and data access restrictions [15]. Here, forest assessment based on open remotely sensed data—recently enhanced by the increased availability of cloud computing environments [16]—overcomes these issues, allowing for the prediction of forest attributes over large temporal and spatial scales [17,18] in a cost-effective way. Yet, despite several satellite missions providing reliable surface reflectance data [19,20] and playing a pivotal role in forest ecosystem monitoring, optical data alone still presents some limitations, such as (i) the spectral reflectance saturation in densely vegetated areas [21], and (ii) a lack of three-dimensional information, which is needed to assess the structure of forests [22,23]. Utilized across a diverse array of platforms, LiDAR (Light Detection and Ranging) has refined the assessment of forest structural attributes by using pulsed laser beams to obtain precise and accurate 3D, geo-located data [24], independently of light conditions [25]. The recent uptake of airborne laser scanner (ALS) technologies has further revolutionized forest structure data acquisition [26], transitioning from experimental to practical applications [27] due to the significant decrease in costs and the increased availability of sensors and acquisition platforms [9]. While ALS complements field measurements by providing three-dimensional information, the combination of optical data and ALS point clouds has shown its effectiveness in several applications compared to using either data source alone [28,29]. In addition, the ability to predict ALS data from optical data presents new opportunities for forest monitoring [30–33], as it allows for data provision in areas where ALS data are currently unavailable, such as tropical evergreen and deciduous forests [34,35]. Indeed, satellite data enables more frequent updates of ALS data, which is crucial in the current context of rapid changes and disturbances driven by climate change. Moreover, having access to comprehensive, wall-to-wall, and annually or sub-annually updated ALS data facilitates the quantification of numerous forest indicators essential for a common forest monitoring system [36]. Indeed, during the last decade, the adoption of ALS technologies has transformed the way forest structure data are captured, becoming a vital tool for forest assessment. Evolving from oceanographic applications, ALS data have been implemented in forest monitoring since the mid-1990s [37,38]. The first reported applications were related to topography, stand height and volume estimation, and single-tree segmentation [39,40]. Since then, ALS technology has been continuously and rapidly developing—along with its application in forestry monitoring [38]—especially in Nordic countries [41]. Overall, the uptake of ALS technologies has revolutionized the capturing of forest structure data, facilitating the assessment of ecosystem services and establishing its role as an essential tool for ecosystem management strategies.

Recently, several authors have analyzed the pivotal role played by ALS data in forest ecosystems, as demonstrated by studies on their applications in aboveground biomass estimation [42] and biodiversity conservation [43]. In fact, the rapid development from scientific tests to operational application [27] was related to decreased associated costs, concurrent with increased sensors and acquisition platform availability. In this context, this study aims at providing a comprehensive review of the most recent (2010–2023) scientific studies addressing the application of ALS data and their derived metrics together with

satellite data in both urban and natural forest ecosystems. Here, we identify emerging trends and knowledge gaps in ALS data applications for forest monitoring. In detail, considering the last decade of research on ALS-based metrics in forest assessment allows this study to identify the most recent applications of this rapidly developing technological tool [44]. Based on the results, we examined the most established ALS-based metrics or ALS-derived forest attributes, the predictor variables used, and the model performances reached, but also the remaining knowledge gaps that need to be addressed by future research.

2. Literature Review

First, we conducted a research in Elsevier's Scopus engine (www.scopus.com) based on the following fixed keywords: "ALS", "LiDAR", "laser scan*", "forest*", "forest variable*", "accurac*", "RMSE", "R^2", and "OA". The asterisk symbol (*) was added to search words that could have multiple spelling variations, allowing for different word endings (e.g., "forest" and "forestry"). Next, we selected only those publications in English, where the keywords were included within their (i) "article title", (ii) "abstract", and (iii) "keywords". The time frame of the literature review was customized to include papers published in the time range from 2010 to 2023. Manuscripts published before 2010 were not considered, as the herein addressed topics are mainly driven by technological advancements and older research may already be obsolete.

Based on this research, we retrieved 4310 peer-reviewed papers, from which self-citations were excluded. We further excluded those documents not classified as "Article", not in the "final publication stage", and not available in "Open Access"; this led to a final set of 2060 documents.

Then, these 2060 articles were ranked based on the ratio between their number of citations and the number of months since the publication date, and the first 500 articles were selected. Finally, the abstracts of the 500 selected articles were carefully read to focus further analysis only on those studies where ALS-based metrics—including both point-cloud-derived metrics (such as height and intensity percentiles) and ALS-derived forest attributes (such as estimates of forest biomass, structure, or biodiversity features)—were (i) followed by some degree of validation and accuracy assessment, either for regression or classification purposes, or (ii) applied to less commonly studied forest attributes (e.g., biodiversity-related variables). As a result, the present study focused on a total of 42 papers, published in peer-reviewed journals from 2010 to 2023 and satisfying the above detailed criteria (Figure 1).

For each paper revised, we extracted (i) the area of interest of the study, (ii) the ALS metrics or ASL-based variables considered for the application, (iii) the average number of laser pulses of the instrument, (iv) the ALS-derived strata such as DTM (Digital Terrain Model), DSM (Digital Surface Model), and CHM (Canopy Height Model) and (v) their spatial resolution, (vi) the forest attributes investigated in the study, (vii) further grouped into eight macro classes (B: biodiversity, BC: biomass and carbon, FC: forest cover, NWFPs: non-wood forest products, S: structure, TS: tree species identification, U: urban environment, and V: volume), (viii) the spatial extent of the study (considering either the grid cell size, the plot size, or the whole study area), (ix) the main methods or algorithm applied, and (x–xiv) the relative accuracy metrics.

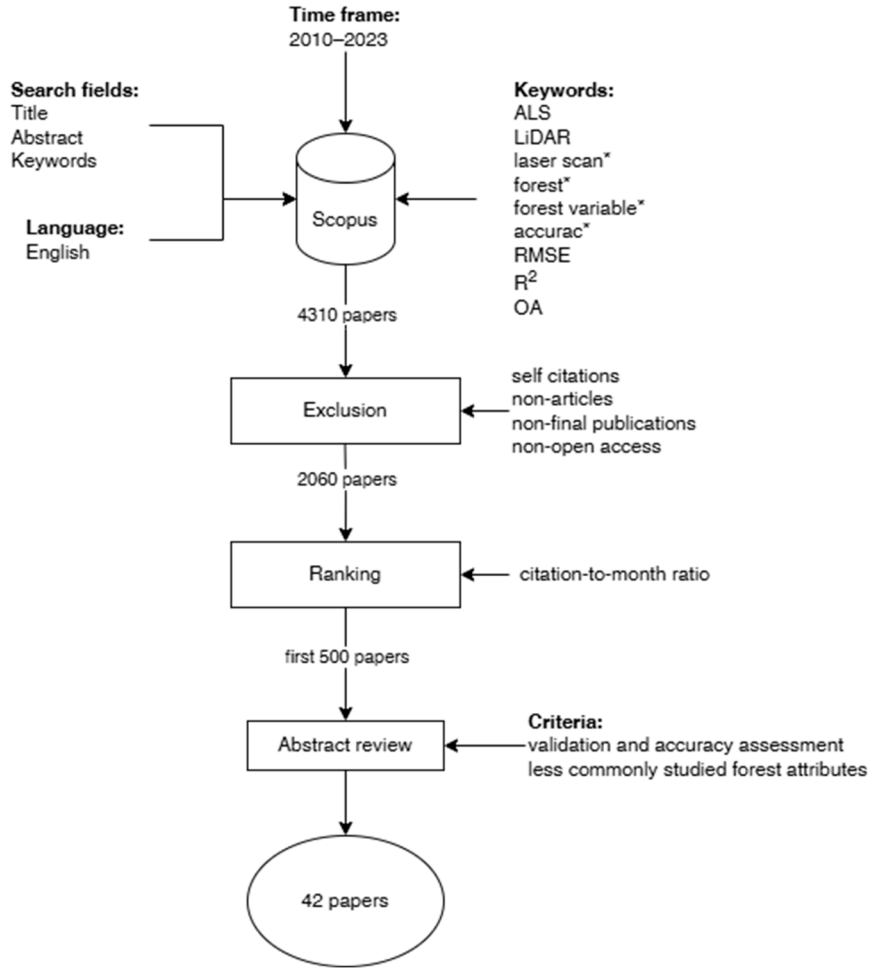

Figure 1. Paper selection process.

3. State of the Art

This study analyzes recent advances in ALS data, analyzing their integration with satellite and field sampling for forest monitoring, showing how this combination provides a detailed, three-dimensional view of forests. The results highlight that integrating ALS with satellite and field data not only enhances the accuracy of estimates, but also enables frequent, large-scale updates, which are crucial for monitoring changes driven by climate changes and human activities, such as forest management practices and urbanization. Thus, this advanced approach thus supports sustainable forest management and contributes to creating key indicators for monitoring frameworks.

3.1. ALS Metrics

The results reported in Table 1 showed how, among the ALS-based metrics, the most implemented were those related to height and intensity (i.e., maximum, minimum, mean, median, SD, variance, percentiles, kurtosis, and skewness). In detail, not only did height metrics consistently correlated with volume, biomass, and structural attributes (i.e., vegetation height, DBH, and basal area), but so did tree species classification [45–47], biodiversity indexes [48]—especially related to birds [49]—and non-wood forest products productivity and yielding [50,51]. As for birds, forest three-dimensional structure has been proven relevant for assessing the habitat quality of other wildlife species, such as bats' occurrence, activity, and abundance [52,53]. Similarly, the signal-return-related metrics proved particularly valuable for biodiversity assessment, including for deadwood analysis [54,55], and for urban forest classification and single-tree assessment [56,57].

Table 1. Results of the peer review process.

Ref	AOI	ALS Metrics/ALS-Based Variables	Average Number of Pulses [n m^{-2}]	Strata Derived	Res [m]	Forest Attributes	Group (s)	Size *	Main Method/ Algorithm	RMSE	RMSE [%]	R^2	OA
[58]	NOR	H (mean, median, SD, 30th percentile, 40–60th relative percentiles, density in the 70–80% above ground threshold) I C_C	7.4	DTM DSM CHM	1	GSV (all species)	V	500–1000 m^2	Most Similar Neighbor Inference	34.56 m^3/ha	17.07		
[59]	SVN	H mean Return (FR, intermediate, only, LR) angle radian ALS intensity	7.5	CHM	1	Canopy cover Vegetation height	TC S	25 m	RF	14.708% 2.054 m			
[60]	FIN	Location (x, y), H (mean, SD range, max, 0–90th percentile, perc of returns below 10–90% of total height); C_A (area of convex hull) C_V (convex hull in 3D) Max crown diameter (ellipse)	2.6	DTM CHM		Height GSV DBH	S V	Single tree	RF	0.30 m 2.30 m^3 0.55 m	10.03 45.77 21.35		
[61]	GBR	FR LR	10–17	DTM DSM CHM	20	Canopy height	TC	20 m	k-NN		28–31		
[54]	FIN	FR LR C_H percentiles C_D percentiles	0.5	DTM	10–20–25–50	Deadwood (CWD volume)	B	10–20–25–50 m sample units					
[62]	ITA	FR LR	8.4	DSM DTM CHM	1 1 10	Volume	V		k-NN	59.2 m^3/ha			
[63]	PAN	Voxels	2	MCH	60	Aboveground Carbon Density	BC	1 ha	R	10.7 MgC/ha			

Table 1. *Cont.*

Ref	AOI	ALS Metrics/ALS-Based Variables	Average Number of Pulses [n m^{-2}]	Strata Derived	Res [m]	Forest Attributes	Group (s)	Size *	Main Method/ Algorithm	RMSE	RMSE [%]	R^2	OA
[64]	CHL	H (percentiles, cv, mean, kurtosis, skewness) C_D	1–3	DTM DSM CHM	1	GSV Canopy height	V TC	0.25 ha	RF	62 m^3/ha 1.7 m	22 7.08	0.81 0.93	
[65]	USA	H (mean, SD, kurtosis, skewness, percentiles, quadratic mean, proportion of points 0–50 m)	2–4	DEM	1	AGB	BC	0.05 ha	R	72.2 Mg/ha		0.83	
[66]	FIN	H (percentiles, mean, SD) C_D	0.6	DTM DSM	1	Dominant height Volume	S V	9 m	k-NN		9.78 19.96		
[67]	USA	Returns (I, identity, coordinates)	0.625	DTM DEM	5	Bird species richness	B	6000 ha	R			0.05–0.22	
[68]	USA	H (max, mean, CV, percentiles) C_C above 2–5 m			18	AGB	BC	-	k-NN			0.74	
[69]	DEU	C_H (mean, SD, max) Penetration rate 5–1 m above ground/10–2 m above ground	25	DTM DSM CHM		Bird species abundance	B	0.01 ha	R		0.07–0.23 (standard error)	0–0.4	
[52]	CHE	Vegetation height (mean, max, SD) Proportion of lower vegetation C_C (mean, SD) Canopy ruggedness Foliage height diversity	7.5			Bats activity	B	1 km^2	GLMM				
[53]	DEU	Roughness (SD) Ground area Deep gap Hits below 5 m Young stands Shrubs North-facing crown area Crown isle Edge Bole zones SD Euphotic zone Regeneration C_H (SD) Entropy (SD) Contrast (SD)	54.74	CHM		Bats activity and species composition	B	1 ha	GLMM				

Table 1. *Cont.*

Ref	AOI	ALS Metrics/ALS-Based Variables	Average Number of Pulses [n m^{-2}]	Strata Derived	Res [m]	Forest Attributes	Group (s)	Size *	Main Method/ Algorithm	RMSE	RMSE [%]	R^2	OA
[70]	CAN	H at which 14 (max canopy height)–25–50–90% of the canopy returns, quadratic mean				AGB	BC	250 m	R	22.2–33.2 Mg/ha		0.64–0.84	
[71]	FIN		1.3	DEM DSM CHM	1	AGB	BC		Stepwise multiple linear regression			0.74	
[72]	CHN	H (10–90%, 25–75th percentiles) Total waveform energy				AGB	BC		RF	9.38–43.81 Mg/ha		0.80–0.90	
[73]	CZE	H (mean, SD) C_D	30–40			Canopy cover	TC		RF	17.38		0.63	
[74]	DEU	H (mean, max, SD) Penetration rate Vertical distribution ratio	25	DTM	100	Fungal fruiting bodies abundance	NWFP	200 m^2				0.23–0.43	
[75]	CAN	H (SD, 50–65–95 percentiles) Canopy relief ratio FR > 1.37 m 0.15–1.37 m proportion of returns	1.4			Berry productivity	NWFP		RF		0–38% variance explained		
[50]	MEX		6			AGB	BC	1 ha		22.22 Mg/ha		0.68	
[51]	FIN	L-moment (and their ratios) C_C	0.91			Silvicultural development classes	TS	255 m^2	RF				72.6
[22]	NOR	H (percentiles) D	7.45			GSV	V	10 m	R	38.4 m^3/ha	17.2	0.83	
[76]	CAN	H (percentiles) Ground returns Canopy returns	1		25	Stand height Crown closure	S TC	20 m	k-NN			0.89 0.63	

Table 1. *Cont.*

Ref	AOI	ALS Metrics/ALS-Based Variables	Average Number of Pulses [n m^{-2}]	Strata Derived	Res [m]	Forest Attributes	Group (s)	Size *	Main Method/ Algorithm	RMSE	RMSE [%]	R^2	OA
[45]	CAN	Ratio of crown area to tree height H (CV, skewness, kurtosis) nH mean and percentiles Ratio of returns in % bins Ratio of FR to all returns Average slope of lines connecting highest returns to others FR mean H/tree H FR median H/tree H FR median H/FR mean H All returns mean H/tree H All returns median H/tree H All returns median H/FR mean H FR median H/all returns mean H FR mean H/all returns mean H FR mean H/2nd returns mean H I	3.3	DTM CHM	1 0.25	Tree species	TS						87
[77]	CAN	Measures of central tendency (mean, median, mode) Measures of dispersion (variance, standard deviation, interquartile range) Percentiles, proportions, and densities of point heights above ground	1.63			Height Basal area GSV Stem density	S V	25 ha		3.08 m 12.56 m^2/ha 115.86 m^3/ha 792.58 trees/ha	17.43 40.76 49.19 66.49	0.76 0.71 0.78 0.26	
[46]	DEU	H-I-E max H-I-E mean H-I-E SD H-I-E CV H-I-E kurtosis H-I-E skewness H-I-E width 25–90th percentiles Mean H of first-or-single returns Percentage of FR-LR > 2 m All returns > 2 m Ratio of crown base H to tree H Ratio of crown volume to crown area Canopy relief ratio	70	DTM	0.5	Tree species	TS		RF				57.1–66.5

Table 1. *Cont.*

Ref	AOI	ALS Metrics/ALS-Based Variables	Average Number of Pulses [n m^{-2}]	Strata Derived	Res [m]	Forest Attributes	Group (s)	Size *	Main Method/ Algorithm	RMSE	RMSE [%]	R^2	OA
[78]	CAN	H (max, percentiles, skewness, SD) Vertical distribution ratio Vertical complexity index CHM metrics	7.3	DTM CHM	1	Lorey's mean height Basal area Gross merchantable volume Total volume AGB	S V BC	20 m	RF			0.94 0.83 0.88 0.91 0.85	
[79]	ESP	Normalized point cloud	0.5			Tree species	TS						83.3
[49]	USA	H (max, mean, SD) Coordinates Canopy models Leaf area density (voxel)	4	DTM DSM	10	Bird species richness proxy	B	20–40-200 m	RF		44.41% variance explained		
[80]	CAN	H (CV, percentiles) Percentage of returns > 2 m	2.8			Lorey's height Basal area GSV AGB	S V BC	30 m	R	2.7 m 6.89 m^2/ha 71.5 m^3/ha 34.4 Mg/ha	24.5 50.7 78.7 65	0.5 0.54 0.49 0.51	
[48]	IRN	H-D (min, max, mean, SD, variance, mode, kurtosis, skewness, percentiles) Penetration of all echoes C_C	4	DTM	1	Menhenick Margalef Simpson Reciprocal of Simpson Shanon-Winer Simpson's evenness	B	0.1 ha	RF		37.8 38.8 27.8 29.3 33.5 24.6		
[81]	FIN	H-I (percentiles, max, min, SD, median, mean, skewness, kurtosis) Density at fixed H Echo class proportion	3.7–4.8	DTM	30	Species-specific GSV	V	30 m			17.8–54.4		

Table 1. *Cont.*

Ref	AOI	ALS Metrics/ALS-Based Variables	Average Number of Pulses [n m^{-2}]	Strata Derived	Res [m]	Forest Attributes	Group (s)	Size *	Main Method/ Algorithm	RMSE	RMSE [%]	R^2	OA
[82]	CAN		0.75–12			Height Basal area GSV	S V			4.9 m 3.8 m^2/ha 224.2 m^3/ha			
[83]	SWE	H C_C I	0.5–1	DEM	2	Berry yield	NWFP	0.25 m^2					
[84]	BRA	C_H LAI	360	DSM DTM CHM	0.2	AGB	BC			7.62 Mg/ha	9	0.82	
[55]	USA	Density percent of FR Percent of second returns Percent of third returns Gap fraction profile Leaf area density Rumple index Entropy Vegetation area index Vertical complexity index Elevation Slope Transformed aspect	4.2			Deadwood (snag characteristics)	B	625 m^2	RF				50–77
[56]	DEU	NR	4.6	CHM	0.5	Urban forest classification Height Crown diameter Crown area	U TS		OBIA R	1.9 m 1.4 m 55.7 m^3		0.79 0.83 0.97	95 5
[57]	CHN	I	230			Urban forest species classification Crown width	U TS		CNN	1 m		0.92	92

Table 1. *Cont.*

Ref	AOI	ALS Metrics/ALS-Based Variables	Average Number of Pulses [n m^{-2}]	Strata Derived	Res [m]	Forest Attributes	Group (s)	Size *	Main Method/ Algorithm	RMSE	RMSE [%]	R^2	OA
[85]	FIN	Points in the 0.2–1 m bin above ground	15			Deadwood	B		CNN	9 m			Precision 31%, recall 30%
[47]	CHN	H (1–99th percentile) I 5th percentile Proportion of points in the 10th bin Mean intensity of single returns Proportion of LR > 2 m Ratio of crown length to average crown Crown diameter SD	320–360	CHM	0.1	Species classification	TS	9 ha					60

* Grid cell size or spatial extent of study area. Abbreviations: C_A (Canopy Area), C_C (Canopy Cover), C_D (Canopy Density), C_H (Canopy Height), C_V (Canopy Volume), CNN (Convolutional Neural Network), DBH (Diameter at Breast Height), DTM (Digital Terrain Model), DSM (Digital Surface Model), E (Echo Width Metrics), F (First Return), GLMM (Generalized Linear Mixed Model), GSV (Growing Stock Volume), H (Height/Height Metrics), I (Intensity Metrics), L (Last Return), MCH (Mean Canopy Profile Height), NR (Number of Returns), OA (Overall Accuracy), OBIA (Object-Based Image Analysis), RMSE (Root Mean Square Error), R (Regression), R^2 (Coefficient of Determination), RF (Random Forest), SD (Standard Deviation), CV (Coefficient of Variation), CHM (Canopy Height Model), Res (Resolution), CWD (Coarse Woody Debris).

Besides the assessment of forest variables, several strata were often derived from ALS data such as Digital Surface Models, Digital Terrain Models, Digital Elevation Models and Canopy Height Models, with spatial resolutions ranging from 0.1 m [47] to 1 ha [74].

Another aspect of ALS data to be considered is pulse density, which refers to the number of emitted laser pulses that intersect a surface per unit area. While strictly influenced by the instrument and acquisition parameters, changes in ALS pulse density can be achieved by modifying flight height or speed [86]. For instance, flying at higher altitudes or speeds can result not only in a reduction in acquisition costs, but also in a lower pulse density [87], resulting in fewer ground returns in areas with dense vegetation [88]. In this analysis, we observed that studies focused on tree species classification [47], particularly in urban settings [57], and on estimating AGB in tropical forests [84] typically utilized higher pulse densities—greater than 100 pulses per square meter. In contrast, research that relied on sparse pulse densities ($\leq$1 pulse/m^2) was mostly conducted in boreal regions like Canada [76], Finland [51,66], and Sweden [83].

3.2. Forest Variables

The most common forest characteristics assessed from ALS data (Figure 2), considering the analyzed papers reported in Table 1, were related to (i) forest structure such as forest height (either at the single tree or the stand level), basal area, DBH, and stand density, and forest height, (ii) volume, and (iii) biomass (also related to carbon content). Along with structural features, ALS-derived forest characteristics were also implemented in the assessment of canopy cover [59,73] and tree species detection in different ecosystems, spanning from the Mediterranean [79], to temperate [46] and boreal biomes [45].

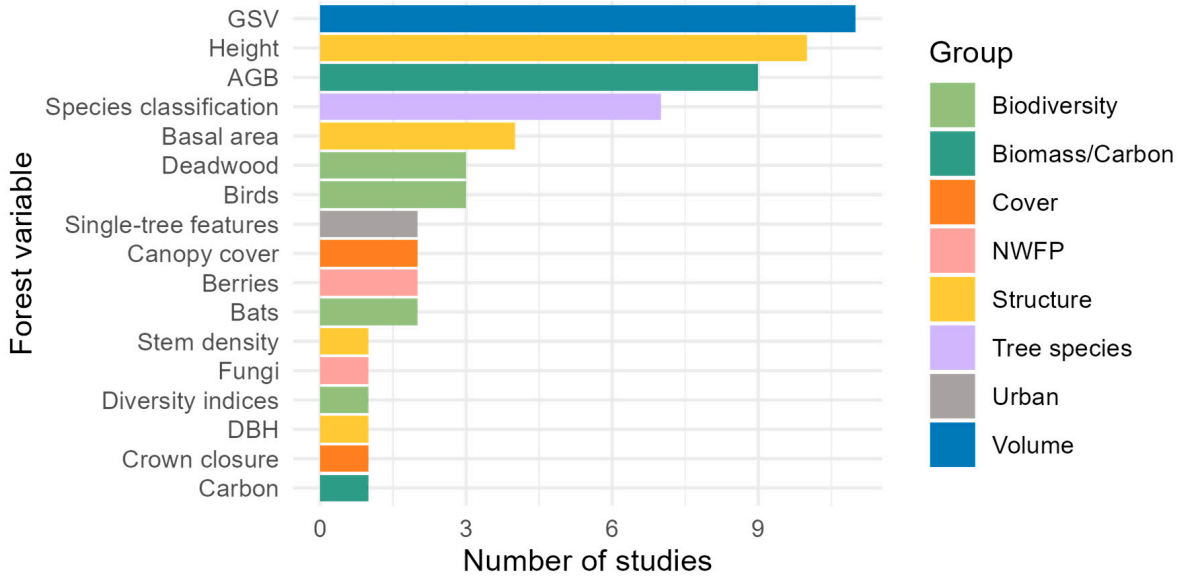

Figure 2. Number of forest variables assessed through ALS-based data, grouped into 8 macro-classes: biodiversity, biomass and carbon, forest cover, non-wood forest products (NWFPs), structure, tree species identification, urban environment and volume.

Moreover, the combination of ALS information with aerial digital photogrammetry allows for the modeling of several tree species diversity indices—i.e., Menhenick, Margalef, Simpson's heterogeneity, reciprocal of Simpson's heterogeneity, Shannon-Winer heterogeneity, and Simpson's evenness—in complex forests ecosystems [48]. In this study, the integration of photogrammetry and ALS data enhanced the model accuracy, resulting in an improvement of approximately 0.2–6.6% in RMSE% and a 4.5% reduction in the relative SD of the differences across species diversity indices. On the other hand, the applications

of ALS data extend to urban environments, given the role that these methodologies can play in accurately assessing vegetation structure properties at different scales. In urban environments, ALS has shown its potential not only in species classification [57], but also in providing the three-dimensional structure of single trees [56].

Besides forest structural characteristics, ALS can play a role in assessing different aspects of forest biodiversity and related ecosystem services. Indeed, the importance of mapping ecosystem services has been widely recognized [89], helping to support sustainable forest management and enabling multiple uses of forest landscapes. In this context, some studies have implemented ALS data to predict the actual yield of edible non-wood forest products such as berries [75,83] or mushrooms [74,90]. Similarly, recent studies have also assessed the capacity of ALS data to differentiate the structural signatures of deadwood—both standing [55] and downed dead trees, especially in old-growth forests [85]—and to optimize deadwood field inventory efficiency, by identifying specific hotspots for coarse woody debris [54]. Along with deadwood, the assessment of biodiversity-related indices through ALS data has been explored, reducing the costs of regular field sampling and increasing its efficiency. Hence, the growing accessibility of ALS data presents a promising opportunity to advance ecological research, especially in the fields of species distribution modeling and habitat quality assessments. In this context, ALS data might be used to better understand the habitat preferences and environmental requirements of different species, leading to more accurate and reliable predictions of their distribution patterns. Additionally, ALS data are instrumental in assessing habitat quality [91]. By capturing high-resolution vegetation structures, ALS data enables the identification of microhabitats, sheltering and foraging spots, and resources that contribute to the overall quality and suitability of certain species. Indeed, the use of ALS data as a valuable proxy for habitat heterogeneity has been largely demonstrated. While previous researchers primarily focused on examining the effectiveness of ALS-derived variables in describing species-environment associations [92,93], over time, the focus shifted to investigating the relationships between vegetation structure and the distribution of individual species, especially concerning birds [49,67,69] and chiropters [52,53]. In detail, previous studies published by [93], and [94], analyze the role that ALS data have been demonstrated to have not only in analyzing trees and forest features, but also in identifying wildlife dynamics in different environments, which are deeply dependent on the structural complexity. Additionally, some studies have explored the variation in the applicability of ALS-derived variables concerning different functional guilds, such as nesting, foraging, and habitat guilds, highlighting that the importance of individual variables and the predictability of species occurrence using vegetation structure differ between these guilds [74].

3.3. Statistical Performance

In the review of studies presented in Table 1, accuracy is primarily reported as the coefficient of determination (R^2), indicating the proportion of variance explained by regression models. Additionally, Root Mean Square Error (RMSE), expressed in either absolute units or as a percentage of the mean in-situ observed value (RMSE%), was frequently employed while overall accuracy (OA) was mainly reported for studies involving classification tasks. Overall, Random Forest (RF) models were the most widely used for both classification and regression tasks. Other commonly used methods were regression and k-NN. RF proved particularly effective in predicting structural attributes, with the highest R^2 values (0.94–0.97) obtained by [56]- for the crown area—and by [78], for Lorey's mean height prediction. On the other hand, the k-NN method was successfully applied in stand height estimation, yielding an R^2 up to 0.89 [76], and a lower RMSE related to structural attributes [66]. Furthermore, ALS data proved to be particularly useful in supporting species

classification—also in urban areas—where they allows models to reach a considerable OA. For instance, in the study carried out by [56] in Dresden (Germany), an OA of 95% was achieved by combining ALS data with multispectral imagery for single tree classification in green and built-up areas. Similar results (OA 92%) were obtained by [57], where hyperspectral and ALS intensity features were combined to identify urban tree species in Hangzhou City (China) through the use of CNN-based segmentation. High-resolution imagery was also implemented in [79], where Pleiades images were combined with low-density ALS data to discriminate pine species in mixed Mediterranean forests, with an OA over 80% in pure stands. Conversely, studies predicting biodiversity variables using ALS data have demonstrated considerable challenges, leading to the lowest performance scores, with R^2 values of up to 0.4 for bird species abundance assessment [69], precision reaching 31% in individual dead tree detection, and a maximum OA of 77% for large snags identification [55]. For these, RF was the most used model, followed by GLMM [52,53].

Finally, Figure 3 provides a summary of the reported RMSE% and R^2 values from the reviewed studies in Table 1. Volume was among the most common forest attributes estimated through ALS data, and it also had the widest range in accuracy. Indeed, the R^2 for the prediction of forest volume ranged from 0.49 to 0.88, whereas for structure, R^2 ranged from 0.26 to 0.94, and from 0.51 to 0.91 for biomass and carbon stock. In contrast, biodiversity and urban variables—while less common—were more consistent in their accuracies, with R^2 ranging from 0.22 to 0.4 and from 0.83 to 0.92, respectively. For RMSE%, volume errors ranged from 10.30 to 78.7%, biomass variables from 9 to 65%, biodiversity from 0.32 to 44.1%, and structural variables from 7.08 to 50.7%.

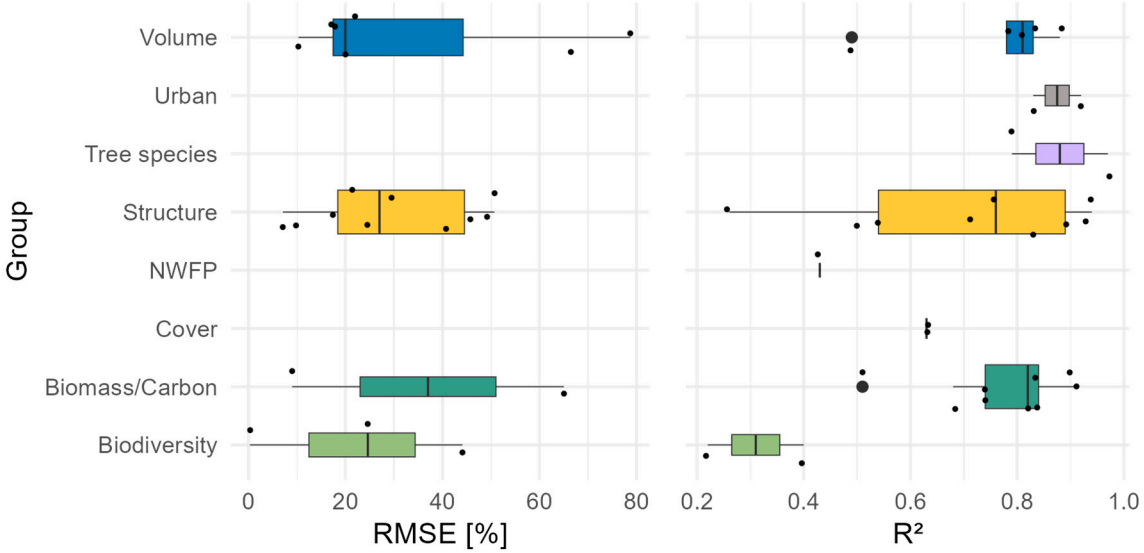

Figure 3. Distribution of RMSE% (on the left)—and R^2 (on the right) of the grouped forest variables for the studies referred to in Table 1, where available.

3.4. Study Areas

From a geographic perspective (Figure 4), most of the studies reviewed were carried out within Europe, the USA, and Canada. In detail, Europe (i.e., Finland, Germany, Norway, Czech Republic, Italy, Slovenia, Spain, Sweden, Switzerland, and the UK) accounted for the most ALS-based studies, with a total of 21 out of 42, followed by the USA and Canada (5 and 8, respectively). South America—i.e., Chile, Brazil, Mexico, and Panama—accounted for almost 10% of the total investigated areas, while the remaining studies were based in China and Iran (three and one, respectively). At the country level, Canada accounted for 19% of the total areas of interest (eight studies), closely followed by Finland (seven

studies), Germany and the United States (both accounting for five studies each), China (three studies), and Norway (two studies). Overall, more than one-third of the studies focused on forests mainly located in boreal ecosystems (15 studies, 35.7% of the total).

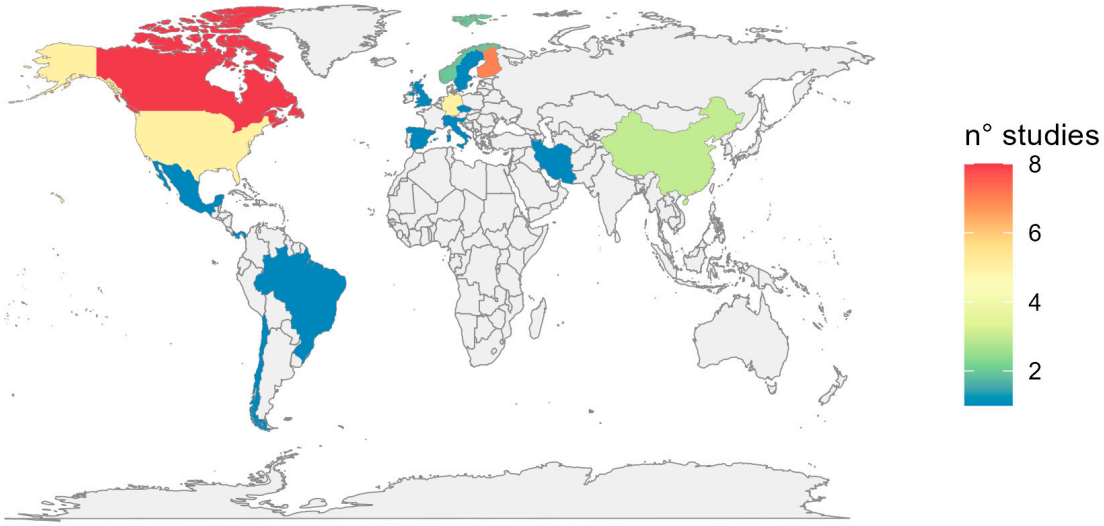

Figure 4. Number of reviewed studies per Country, based on the location of the area of interest.

4. Take Home Messages

Based on this study, several conclusions can be drawn. First, the findings of this analysis underscore the significant role of ALS data in assessing forest characteristics, especially through height and intensity metrics. Indeed, ALS enables accurate estimates of essential variables such as biomass, biodiversity, and forest structure, overcoming the limitations of optical data alone [95]—which are not able to capture the vertical structure—and traditional in-situ samplings [55], especially in terms of area coverage [96,97]. Studies on the ability of ALS data to profile the three dimensions of forests suggested that this technology could support the assessment of forest biodiversity—especially regarding larger elements, such as snags [55]—aiding in capturing information on the composition and structure of trophic niches [98]. Despite providing reliable information on forest vertical characteristics and heterogeneity—which can be positively correlated to the diversity of species [99,100]—ALS data alone presented limitations, especially regarding complex forest elements like smaller deadwood [85], and in the detectability of species and characteristics related to forest understory [101,102], especially in dense canopy conditions [49]. Indeed, due to their inherent characteristics, biodiversity-relevant ALS metrics are often case-specific, as there is no single general metric suitable for all ALS-based forest biodiversity assessments (e.g., [54,55,85]). While promising, species richness and abundance metrics yielded moderate fits among the reported studies, perhaps due to their complex non-linear relationship with ALS predictors [67], or due to the low variability within small study areas [103]. Perhaps, whether ALS data are collected under leaf-on, or leaf-off conditions may further influence the observed correlations, especially when analyzing seasonal organisms [67]. In this context, integrating ALS data with various information sources—such as in-situ measurements [55], terrestrial scanning [104], or additional remote sensing spectral data [48]—might enhance regular and comprehensive analyses, helping to overcome the limitations posed by the absence of multi-temporal ALS data. This has been proven effective in urban environments, where the integration of ALS data with multispectral imagery [56] and hyperspectral features [57] achieved high accuracies for tree species identification.

Second, the analysis reveals that higher pulse densities are pivotal for accurate tree species classification and biomass estimation, especially in dense tropical forests [105,106]. Previous studies have shown that low pulse densities (>0.5 pulses/m^2) are necessary for reliable canopy metrics and digital terrain models in tropical rainforests [107,108], while higher pulse densities (>15 pulses/m^2) were required for estimating leaf area density profiles in dense tropical forests [109]. The effects of a reduced pulse density are more pronounced in areas with steep slopes and dense vegetation, leading to poor ground surface identification and under-sampling of the canopy profile [105,108]. However, lower pulse densities can still provide accurate biomass change estimates if a high-quality digital terrain model is available from at least one high-density survey [105]. Here, the correct identification of the ground surface [108]—and, thus, the creation of an efficient DTM [105]—is crucial not only for forest metrics' estimation (such as carbon and biomass) [110], but also for detecting selective logging activities [111]. On the other hand, high point densities require high acquisition costs and longer flight times [87], compared to low-density data. To address this gap, the integration of ALS data with other sources of information may enhance the ability to estimate biomass and carbon content in tropical regions, providing spatially explicit information across otherwise inaccessible landscapes, and decreasing reliance on extensive field sampling [112]. Here, ALS data could overcome the limitations of optical remote sensing—due to complex canopy cover, and the presence of clouds—and field-based observation, allowing for the retrieval of the three-dimensional structures of tropical ecosystems [113]. Recent applications of ALS data have been proven effective in capturing trees' height, even in dense and stratified canopy conditions [102]. This approach significantly reduces the costs associated with in-situ measurements in challenging environments while also mitigating inaccuracies, particularly in tree height estimation [102]. Furthermore, the fusion of ALS data with other sources of information (i.e., hyperspectral imagery) could complement the structural information provided by ALS [114,115]. Similarly, the optimization of acquisition time, perhaps by avoiding midday hours, can enhance both ground and canopy detection in dense tropical forests [116].

Third, this study identified a geographical bias in ALS research, predominantly concentrated in Europe and North America, particularly within boreal ecosystems. This underscores the necessity for further expanding studies into tropical and subtropical regions, where ALS has the potential to yield valuable insights into biodiversity and ecosystem services. Here, the scattered availability of ground-based data may hinder the training of algorithms and the validation of derived products [117,118]. To address this issue, recent studies emphasize the importance of calibrating ALS data locally using permanent sampling plots [119], or to prioritizing the establishment of supersites with long-term observation capacity [119]. On the other hand, open data policies can significantly impact the expansion of ALS data application in forestry [96], especially in understudied regions. Along with international missions—such as ICESat-2 and GEDI [120,121]—several national and regional datasets became openly accessible in recent years (e.g., [122,123]), broadening the potential to utilize ALS data for extensive forest monitoring applications [112] and to spatially extend important forest attributes to areas lacking current inventories (e.g., [124]). This expansion would enhance the relevance and benefits of ALS data for forest management and conservation initiatives, by optimizing carbon stock and biomass quantification [125].

In conclusion, over recent decades, ALS data have significantly advanced the assessment of forest features. In addition, while this study considers the most recent applications of ALS in the forestry sector, ALS technology had been operationally applied to forest research for more than half a decade before 2010, for instance, to assess forest structural variables such as tree height, mean diameter, basal area, stem number, and timber vol-

ume [40,126,127], above- and below-ground biomass [128,129], and carbon stock [130]. Still, limitations persist, particularly in detecting understory elements, and in ensuring comprehensive spatial coverage. These limitations may be addressed through the integration of ALS data with other data sources, including in-situ measurements (especially regarding biodiversity variables) and satellite imagery. However, the high cost of ALS data acquisition, especially when higher pulse densities are required, remains a challenge. Hence, the geographical concentration of ALS research in Europe and North America underscores the need for increased studies in tropical and subtropical regions, where ecosystems play a critical role in carbon sequestration and biodiversity conservation. Nevertheless, ongoing technological advancements, decreasing ALS costs, and the expansion of open data initiatives present promising opportunities to extend the application of ALS in forest monitoring and management. These advancements are expected to enhance the ability to assess and conserve carbon stocks, biodiversity, and forest structure across diverse ecosystems globally.

Author Contributions: Conceptualization, S.F and C.B.; methodology, C.B. and S.F.; investigation, C.B.; writing—original draft preparation, C.B. and S.F.; writing—review and editing, C.B., S.F, G.D., R.V. and G.C.; supervision, G.C. All authors have read and agreed to the published version of the manuscript.

Funding: This research received no external funding.

Data Availability Statement: These data were derived from the following resources available in the public domain: www.scopus.com.

Acknowledgments: This article was carried out in the framework of the following projects: EFINET "European Forest Information Network" funded by the European Forest Institute, Network Fund G-01-2021. FORWARDS. H2020 project funded by the European Commission, number 101084481 call HORIZON-CL6-2022-CLIMATE-01-05. MONIFUN. H2020 project funded by the European Commission, number 101134991 call HORIZON-CL6-2023-CircBio-01-14. NextGenCarbon. H2020 project funded by the European Commission, number 101184989 call HORIZON-CL5-2024-D1-01-07. SUPERB. H2020 project funded by the European Commission, number 101036849 call LC-GD-7-1-2020; MULTIFOR "Multi-scale observations to predict Forest response to pollution and climate change" PRIN 2020 Research Project of National. Relevance funded by the Italian Ministry of University and Research (prot. 2020E52THS).

Conflicts of Interest: The authors declare no conflicts of interest.

References

1. Friedlingstein, P.; Jones, M.W.; O'Sullivan, M.; Andrew, R.M.; Bakker, D.C.E.; Hauck, J.; Le Quéré, C.; Peters, G.P.; Peters, W.; Pongratz, J. Global Carbon Budget 2021. *Earth Syst. Sci. Data* **2022**, *14*, 1917–2005. [CrossRef]
2. Francini, S.; Chirici, G.; Chiesi, L.; Costa, P.; Caldarelli, G.; Mancuso, S. Global Spatial Assessment of Potential for New Peri-Urban Forests to Combat Climate Change. *Nat. Cities* **2024**, *1*, 286–294. [CrossRef]
3. Oliveira, M.; Santagata, R.; Kaiser, S.; Liu, Y.; Vassillo, C.; Ghisellini, P.; Liu, G.; Ulgiati, S. Socioeconomic and Environmental Benefits of Expanding Urban Green Areas: A Joint Application of i-Tree and LCA Approaches. *Land* **2022**, *11*, 2106. [CrossRef]
4. Sacchelli, S.; Borghi, C.; Fratini, R.; Bernetti, I. Assessment and Valorization of Non-Wood Forest Products in Europe: A Quantitative Literature Review. *Sustainability* **2021**, *13*, 3533. [CrossRef]
5. Manes, F.; Marando, F.; Capotorti, G.; Blasi, C.; Salvatori, E.; Fusaro, L.; Ciancarella, L.; Mircea, M.; Marchetti, M.; Chirici, G.; et al. Regulating Ecosystem Services of Forests in Ten Italian Metropolitan Cities: Air Quality Improvement by PM_{10} and O_3 Removal. *Ecol. Indic.* **2016**, *67*, 425–440. [CrossRef]
6. Sannigrahi, S.; Chakraborti, S.; Joshi, P.K.K.; Keesstra, S.; Sen, S.; Paul, S.K.K.; Kreuter, U.; Sutton, P.C.C.; Jha, S.; Dang, K.B.B. Ecosystem Service Value Assessment of a Natural Reserve Region for Strengthening Protection and Conservation. *J. Environ. Manag.* **2019**, *244*, 208–227. [CrossRef]
7. Seidl, R.; Thom, D.; Kautz, M.; Martin-Benito, D.; Peltoniemi, M.; Vacchiano, G.; Wild, J.; Ascoli, D.; Petr, M.; Honkaniemi, J.; et al. Forest Disturbances under Climate Change. *Nat. Clim. Chang.* **2017**, *7*, 395–402. [CrossRef]

8. Duncanson, L.; Armston, J.; Disney, M.; Avitabile, V.; Barbier, N.; Calders, K.; Carter, S.; Chave, J.; Herold, M.; Crowther, T.W.; et al. The Importance of Consistent Global Forest Aboveground Biomass Product Validation. *Surv. Geophys.* **2019**, *40*, 979–999. [CrossRef]
9. Coops, N.C.; Tompalski, P.; Goodbody, T.R.H.; Queinnec, M.; Luther, J.E.; Bolton, D.K.; White, J.C.; Wulder, M.A.; van Lier, O.R.; Hermosilla, T. Modelling Lidar-Derived Estimates of Forest Attributes over Space and Time: A Review of Approaches and Future Trends. *Remote Sens. Environ.* **2021**, *260*, 112477. [CrossRef]
10. Breidenbach, J.; McRoberts, R.E.; Alberdi, I.; Antón-Fernández, C.; Tomppo, E. A Century of National Forest Inventories—Informing Past, Present and Future Decisions. *For. Ecosyst.* **2021**, *8*, 36. [CrossRef]
11. Borghi, C.; Francini, S.; McRoberts, R.E.; Parisi, F.; Lombardi, F.; Nocentini, S.; Maltoni, A.; Travaglini, D.; Chirici, G. Country-Wide Assessment of Biodiversity, Naturalness, and Old-Growth Status Using National Forest Inventory Data. *Eur. J. For. Res.* **2023**, *143*, 271–303. [CrossRef]
12. Tomppo, E.; Gschwantner, T.; Lawrence, M.; McRoberts, R.E. *National Forest Inventories: Pathways for Common Reporting*; Tomppo, E., Gschwantner, T., Lawrence, M., McRoberts, R.E., Eds.; Springer: Dordrecht, The Netherlands, 2010; ISBN 9789048132324.
13. Gschwantner, T.; Alberdi, I.; Balázs, A.; Bauwens, S.; Bender, S.; Borota, D.; Bosela, M.; Bouriaud, O.; Cañellas, I.; Donis, J.; et al. Harmonisation of Stem Volume Estimates in European National Forest Inventories. *Ann. For. Sci.* **2019**, *76*, 24. [CrossRef]
14. Vidal, C.; Alberdi, I.; Hernández, L.; Redmond, J.J. *National Forest Inventories*; Vidal, C., Alberdi, I.A., Hernández Mateo, L., Redmond, J.J., Eds.; Springer International Publishing: Cham, Switzerland, 2016; Volume 10, ISBN 978-3-319-44014-9.
15. Gessler, A.; Schaub, M.; Bose, A.; Trotsiuk, V.; Valbuena, R.; Chirici, G.; Buchmann, N. Finding the Balance between Open Access to Forest Data While Safeguarding the Integrity of National Forest Inventory-Derived Information. *New Phytol.* **2024**, *242*, 344–346. [CrossRef]
16. Gorelick, N.; Hancher, M.; Dixon, M.; Ilyushchenko, S.; Thau, D.; Moore, R. Google Earth Engine: Planetary-Scale Geospatial Analysis for Everyone. *Remote Sens. Environ.* **2017**, *202*, 18–27. [CrossRef]
17. Francini, S.; Hermosilla, T.; Coops, N.C.; Wulder, M.A.; White, J.C.; Chirici, G. An Assessment Approach for Pixel-Based Image Composites. *ISPRS J. Photogramm. Remote Sens.* **2023**, *202*, 1–12. [CrossRef]
18. Vangi, E.; D'Amico, G.; Francini, S.; Borghi, C.; Giannetti, F.; Corona, P.; Marchetti, M.; Travaglini, D.; Pellis, G.; Vitullo, M.; et al. Large-Scale High-Resolution Yearly Modeling of Forest Growing Stock Volume and above-Ground Carbon Pool. *Environ. Model. Softw.* **2023**, *159*, 105580. [CrossRef]
19. Wulder, M.A.; Loveland, T.R.; Roy, D.P.; Crawford, C.J.; Masek, J.G.; Woodcock, C.E.; Allen, R.G.; Anderson, M.C.; Belward, A.S.; Cohen, W.B.; et al. Current Status of Landsat Program, Science, and Applications. *Remote Sens. Environ.* **2019**, *225*, 127–147. [CrossRef]
20. Claverie, M.; Ju, J.; Masek, J.G.; Dungan, J.L.; Vermote, E.F.; Roger, J.C.; Skakun, S.V.; Justice, C. The Harmonized Landsat and Sentinel-2 Surface Reflectance Data Set. *Remote Sens. Environ.* **2018**, *219*, 145–161. [CrossRef]
21. Mutanga, O.; Masenyama, A.; Sibanda, M. Spectral Saturation in the Remote Sensing of High-Density Vegetation Traits: A Systematic Review of Progress, Challenges, and Prospects. *ISPRS J. Photogramm. Remote Sens.* **2023**, *198*, 297–309. [CrossRef]
22. Puliti, S.; Saarela, S.; Gobakken, T.; Ståhl, G.; Næsset, E. Combining UAV and Sentinel-2 Auxiliary Data for Forest Growing Stock Volume Estimation through Hierarchical Model-Based Inference. *Remote Sens. Environ.* **2018**, *204*, 485–497. [CrossRef]
23. Lefsky, M.A.; Cohen, W.B.; Parker, G.G.; Harding, D.J. Lidar Remote Sensing for Ecosystem Studies. *Bioscience* **2002**, *52*, 19–30. [CrossRef]
24. Andersen, H.-E.; Reutebuch, S.E.; McGaughey, R.J. Active Remote Sensing. In *Computer Applications in Sustainable Forest Management: Including Perspectives on Collaboration and Integration*; Springer: Berlin/Heidelberg, Germany, 2006; pp. 43–66.
25. Shan, J.; Toth, C.K. *Topographic Laser Ranging and Scanning: Principles and Processing*; CRC press: Boca Raton, FL, USA, 2018; ISBN 1498772285.
26. May, P.B.; Dubayah, R.O.; Bruening, J.M.; Gaines, G.C. Connecting Spaceborne Lidar with NFI Networks: A Method for Improved Estimation of Forest Structure and Biomass. *Int. J. Appl. Earth Obs. Geoinf.* **2024**, *129*, 103797. [CrossRef]
27. Nelson, R. How Did We Get Here? An Early History of Forestry Lidar 1. *Can. J. Remote Sens.* **2013**, *39*, S6–S17. [CrossRef]
28. Camarretta, N.; Harrison, P.A.; Bailey, T.; Potts, B.; Lucieer, A.; Davidson, N.; Hunt, M. Monitoring Forest Structure to Guide Adaptive Management of Forest Restoration: A Review of Remote Sensing Approaches. *New For.* **2020**, *51*, 573–596. [CrossRef]
29. Kukkonen, M.; Korhonen, L.; Maltamo, M.; Suvanto, A.; Packalen, P. How Much Can Airborne Laser Scanning Based Forest Inventory by Tree Species Benefit from Auxiliary Optical Data? *Int. J. Appl. Earth Obs. Geoinf.* **2018**, *72*, 91–98. [CrossRef]
30. Matasci, G.; Hermosilla, T.; Wulder, M.A.; White, J.C.; Coops, N.C.; Hobart, G.W.; Bolton, D.K.; Tompalski, P.; Bater, C.W. Three Decades of Forest Structural Dynamics over Canada's Forested Ecosystems Using Landsat Time-Series and Lidar Plots. *Remote Sens. Environ.* **2018**, *216*, 697–714. [CrossRef]
31. Tanase, M.A.; Mihai, M.C.; Miguel, S.; Cantero, A.; Tijerin, J.; Ruiz-Benito, P.; Domingo, D.; Garcia-Martin, A.; Aponte, C.; Lamelas, M.T. Long-Term Annual Estimation of Forest above Ground Biomass, Canopy Cover, and Height from Airborne and Spaceborne Sensors Synergies in the Iberian Peninsula. *Environ. Res.* **2024**, *259*, 119432. [CrossRef]

32. Wulder, M.A.; White, J.C.; Bater, C.W.; Coops, N.C.; Hopkinson, C.; Chen, G. Lidar Plots—A New Large-Area Data Collection Option: Context, Concepts, and Case Study. *Can. J. Remote Sens.* **2012**, *38*, 600–618. [CrossRef]
33. Wang, D.; Wan, B.; Liu, J.; Su, Y.; Guo, Q.; Qiu, P.; Wu, X. Estimating Aboveground Biomass of the Mangrove Forests on Northeast Hainan Island in China Using an Upscaling Method from Field Plots, UAV-LiDAR Data and Sentinel-2 Imagery. *Int. J. Appl. Earth Obs. Geoinf.* **2020**, *85*, 101986. [CrossRef]
34. Staben, G.; Lucieer, A.; Scarth, P. Modelling LiDAR Derived Tree Canopy Height from Landsat TM, ETM+ and OLI Satellite Imagery—A Machine Learning Approach. *Int. J. Appl. Earth Obs. Geoinf.* **2018**, *73*, 666–681. [CrossRef]
35. Ota, T.; Kajisa, T.; Mizoue, N.; Yoshida, S.; Takao, G.; Hirata, Y.; Furuya, N.; Sano, T.; Ponce-Hernandez, R.; Ahmed, O.S.; et al. Estimating Aboveground Carbon Using Airborne LiDAR in Cambodian Tropical Seasonal Forests for REDD+ Implementation. *J. For. Res.* **2015**, *20*, 484–492. [CrossRef]
36. Ferretti, M.; Fischer, C.; Gessler, A.; Graham, C.; Meusburger, K.; Abegg, M.; Bebi, P.; Bergamini, A.; Brockerhoff, E.G.; Brunner, I.; et al. Advancing Forest Inventorying and Monitoring. *Ann. For. Sci.* **2024**, *81*, 6. [CrossRef]
37. Vauhkonen, J.; Maltamo, M.; McRoberts, R.E.; Næsset, E. Introduction to Forestry Applications of Airborne Laser Scanning. In *Forestry Applications of Airborne Laser Scanning*; Springer: Berlin/Heidelberg, Germany, 2014; pp. 1–16.
38. Balenović, I.; Alberti, G.; Marjanović, H. Airborne Laser Scanning—The Status and Perspectives for the Application in the South-East European Forestry. *South-East Eur. For.* **2013**, *4*, 59–79. [CrossRef]
39. Hyyppa, J.; Hyyppa, H.; Litkey, P.; Yu, X.; Haggren, H.; Rönnholm, P.; Pyysalo, U.; Pitkänen, J.; Maltamo, M. Algorithms and Methods of Airborne Laser Scanning for Forest Measurements. *Int. Arch. Photogramm. Remote Sens. Spat. Inf. Sci.* **2000**, *36*, 82–89.
40. Lim, K.; Treitz, P.; Wulder, M.; St-Onge, B.; Flood, M. LiDAR Remote Sensing of Forest Structure. *Prog. Phys. Geogr. Earth Environ.* **2003**, *27*, 88–106. [CrossRef]
41. Hyyppä, J.; Holopainen, M.; Olsson, H. Laser Scanning in Forests. *Remote Sens.* **2012**, *4*, 2919–2922. [CrossRef]
42. Tian, L.; Wu, X.; Tao, Y.; Li, M.; Qian, C.; Liao, L.; Fu, W. Review of Remote Sensing-Based Methods for Forest Aboveground Biomass Estimation: Progress, Challenges, and Prospects. *Forests* **2023**, *14*, 1086. [CrossRef]
43. Toivonen, J.; Kangas, A.; Maltamo, M.; Kukkonen, M.; Packalen, P. Assessing Biodiversity Using Forest Structure Indicators Based on Airborne Laser Scanning Data. *For. Ecol. Manag.* **2023**, *546*, 121376. [CrossRef]
44. Nitoslawski, S.A.; Wong-Stevens, K.; Steenberg, J.W.N.; Witherspoon, K.; Nesbitt, L.; Konijnendijk van den Bosch, C.C. The Digital Forest: Mapping a Decade of Knowledge on Technological Applications for Forest Ecosystems. *Earth's Futur.* **2021**, *9*, e2021EF002123. [CrossRef]
45. Budei, B.C.; St-Onge, B. Variability of Multispectral Lidar 3D and Intensity Features with Individual Tree Height and Its Influence on Needleleaf Tree Species Identification. *Can. J. Remote Sens.* **2018**, *44*, 263–286. [CrossRef]
46. Shi, Y.; Wang, T.; Skidmore, A.K.; Heurich, M. Important LiDAR Metrics for Discriminating Forest Tree Species in Central Europe. *ISPRS J. Photogramm. Remote Sens.* **2018**, *137*, 163–174. [CrossRef]
47. Quan, Y.; Li, M.; Hao, Y.; Liu, J.; Wang, B. Tree Species Classification in a Typical Natural Secondary Forest Using UAV-Borne LiDAR and Hyperspectral Data. *GIScience Remote Sens.* **2023**, *60*, 2171706. [CrossRef]
48. Mohammadi, J.; Shataee, S.; Næsset, E. Modeling Tree Species Diversity by Combining ALS Data and Digital Aerial Photogrammetry. *Sci. Remote Sens.* **2020**, *2*, 100011. [CrossRef]
49. Carrasco, L.; Giam, X.; Papeş, M.; Sheldon, K. Metrics of Lidar-Derived 3D Vegetation Structure Reveal Contrasting Effects of Horizontal and Vertical Forest Heterogeneity on Bird Species Richness. *Remote Sens.* **2019**, *11*, 743. [CrossRef]
50. Urbazaev, M.; Thiel, C.; Cremer, F.; Dubayah, R.; Migliavacca, M.; Reichstein, M.; Schmullius, C. Estimation of Forest Aboveground Biomass and Uncertainties by Integration of Field Measurements, Airborne LiDAR, and SAR and Optical Satellite Data in Mexico. *Carbon Balance Manag.* **2018**, *13*, 5. [CrossRef]
51. Valbuena, R.; Maltamo, M.; Packalen, P. Classification of Multilayered Forest Development Classes from Low-Density National Airborne Lidar Datasets. *Forestry* **2016**, *89*, 392–401. [CrossRef]
52. Froidevaux, J.S.P.; Zellweger, F.; Bollmann, K.; Jones, G.; Obrist, M.K. From Field Surveys to LiDAR: Shining a Light on How Bats Respond to Forest Structure. *Remote Sens. Environ.* **2016**, *175*, 242–250. [CrossRef]
53. Jung, K.; Kaiser, S.; Böhm, S.; Nieschulze, J.; Kalko, E.K.V. Moving in Three Dimensions: Effects of Structural Complexity on Occurrence and Activity of Insectivorous Bats in Managed Forest Stands. *J. Appl. Ecol.* **2012**, *49*, 523–531. [CrossRef]
54. Pesonen, A.; Kangas, A.; Maltamo, M.; Packalén, P. Effects of Auxiliary Data Source and Inventory Unit Size on the Efficiency of Sample-Based Coarse Woody Debris Inventory. *For. Ecol. Manag.* **2010**, *259*, 1890–1899. [CrossRef]
55. Stitt, J.M.; Hudak, A.T.; Silva, C.A.; Vierling, L.A.; Vierling, K.T. Evaluating the Use of Lidar to Discern Snag Characteristics Important for Wildlife. *Remote Sens.* **2022**, *14*, 720. [CrossRef]
56. Münzinger, M.; Prechtel, N.; Behnisch, M. Mapping the Urban Forest in Detail: From LiDAR Point Clouds to 3D Tree Models. *Urban For. Urban Green.* **2022**, *74*, 127637. [CrossRef]

57. Gong, Y.; Zhu, D.; Li, X.; Lv, L.; Zhang, B.; Xuan, J.; Du, H. Using UAV LiDAR Intensity Frequency and Hyperspectral Features to Improve the Accuracy of Urban Tree Species Classification. *IEEE J. Sel. Top. Appl. Earth Obs. Remote Sens.* **2023**, *17*, 2849–2865. [CrossRef]
58. Breidenbach, J.; Nothdurft, A.; Kändler, G. Comparison of Nearest Neighbour Approaches for Small Area Estimation of Tree Species-Specific Forest Inventory Attributes in Central Europe Using Airborne Laser Scanner Data. *Eur. J. For. Res.* **2010**, *129*, 833–846. [CrossRef]
59. Stojanova, D.; Panov, P.; Gjorgjioski, V.; Kobler, A.; Džeroski, S. Estimating Vegetation Height and Canopy Cover from Remotely Sensed Data with Machine Learning. *Ecol. Inform.* **2010**, *5*, 256–266. [CrossRef]
60. Yu, X.; Hyyppä, J.; Vastaranta, M.; Holopainen, M.; Viitala, R. Predicting Individual Tree Attributes from Airborne Laser Point Clouds Based on the Random Forests Technique. *ISPRS J. Photogramm. Remote Sens.* **2011**, *66*, 28–37. [CrossRef]
61. Mcinerney, D.O.; Suarez-Minguez, J.; Valbuena, R.; Nieuwenhuis, M. Forest Canopy Height Retrieval Using LiDAR Data, Medium-Resolution Satellite Imagery and KNN Estimation in Aberfoyle, Scotland. *Forestry* **2010**, *83*, 195–206. [CrossRef]
62. Maselli, F.; Chiesi, M.; Montaghi, A.; Pranzini, E. Use of ETM+ Images to Extend Stem Volume Estimates Obtained from LiDAR Data. *ISPRS J. Photogramm. Remote Sens.* **2011**, *66*, 662–671. [CrossRef]
63. Mascaro, J.; Detto, M.; Asner, G.P.; Muller-Landau, H.C. Evaluating Uncertainty in Mapping Forest Carbon with Airborne LiDAR. *Remote Sens. Environ.* **2011**, *115*, 3770–3774. [CrossRef]
64. Cartus, O.; Kellndorfer, J.; Rombach, M.; Walker, W. Mapping Canopy Height and Growing Stock Volume Using Airborne Lidar, ALOS PALSAR and Landsat ETM+. *Remote Sens.* **2012**, *4*, 3320–3345. [CrossRef]
65. Chen, Q.; Vaglio Laurin, G.; Battles, J.J.; Saah, D. Integration of Airborne Lidar and Vegetation Types Derived from Aerial Photography for Mapping Aboveground Live Biomass. *Remote Sens. Environ.* **2012**, *121*, 108–117. [CrossRef]
66. Villikka, M.; Packalén, P.; Maltamo, M. The Suitability of Leaf-off Airborne Laser Scanning Data in an Area-Based Forest Inventory of Coniferous and Deciduous Trees. *Silva Fenn.* **2012**, *46*, 68. [CrossRef]
67. Lesak, A.A.; Radeloff, V.C.; Hawbaker, T.J.; Pidgeon, A.M.; Gobakken, T.; Contrucci, K. Modeling Forest Songbird Species Richness Using LiDAR-Derived Measures of Forest Structure. *Remote Sens. Environ.* **2011**, *115*, 2823–2835. [CrossRef]
68. Andersen, H.-E.; Strunk, J.; Temesgen, H.; Atwood, D.; Winterberger, K. Using Multilevel Remote Sensing and Ground Data to Estimate Forest Biomass Resources in Remote Regions: A Case Study in the Boreal Forests of Interior Alaska. *Can. J. Remote Sens.* **2011**, *37*, 596–611. [CrossRef]
69. Müller, J.; Moning, C.; Bässler, C.; Heurich, M.; Brandl, R. Using Airborne Laser Scanning to Model Potential Abundance and Assemblages of Forest Passerines. *Basic Appl. Ecol.* **2009**, *10*, 671–681. [CrossRef]
70. Margolis, H.A.; Nelson, R.F.; Montesano, P.M.; Beaudoin, A.; Sun, G.; Andersen, H.-E.; Wulder, M.A. Combining Satellite Lidar, Airborne Lidar, and Ground Plots to Estimate the Amount and Distribution of Aboveground Biomass in the Boreal Forest of North America. *Can. J. For. Res.* **2015**, *45*, 838–855. [CrossRef]
71. Badreldin, N.; Sanchez-Azofeifa, A. Estimating Forest Biomass Dynamics by Integrating Multi-Temporal Landsat Satellite Images with Ground and Airborne LiDAR Data in the Coal Valley Mine, Alberta, Canada. *Remote Sens.* **2015**, *7*, 2832–2849. [CrossRef]
72. Chi, H.; Sun, G.; Huang, J.; Guo, Z.; Ni, W.; Fu, A. National Forest Aboveground Biomass Mapping from ICESat/GLAS Data and MODIS Imagery in China. *Remote Sens.* **2015**, *7*, 5534–5564. [CrossRef]
73. Latifi, H.; Heurich, M.; Hartig, F.; Müller, J.; Krzystek, P.; Jehl, H.; Dech, S. Estimating Over- and Understorey Canopy Density of Temperate Mixed Stands by Airborne LiDAR Data. *Forestry* **2016**, *89*, 69–81. [CrossRef]
74. Peura, M.; Silveyra Gonzalez, R.; Müller, J.; Heurich, M.; Vierling, L.A.; Mönkkönen, M.; Bässler, C. Mapping a 'Cryptic Kingdom': Performance of Lidar Derived Environmental Variables in Modelling the Occurrence of Forest Fungi. *Remote Sens. Environ.* **2016**, *186*, 428–438. [CrossRef]
75. Barber, Q.E.; Bater, C.W.; Braid, A.C.R.; Coops, N.C.; Tompalski, P.; Nielsen, S.E. Airborne Laser Scanning for Modelling Understory Shrub Abundance and Productivity. *For. Ecol. Manag.* **2016**, *377*, 46–54. [CrossRef]
76. Mahoney, C.; Hall, R.; Hopkinson, C.; Filiatrault, M.; Beaudoin, A.; Chen, Q. A Forest Attribute Mapping Framework: A Pilot Study in a Northern Boreal Forest, Northwest Territories, Canada. *Remote Sens.* **2018**, *10*, 1338. [CrossRef]
77. Tompalski, P.; Coops, N.; Marshall, P.; White, J.; Wulder, M.; Bailey, T. Combining Multi-Date Airborne Laser Scanning and Digital Aerial Photogrammetric Data for Forest Growth and Yield Modelling. *Remote Sens.* **2018**, *10*, 347. [CrossRef]
78. Luther, J.E.; Fournier, R.A.; van Lier, O.R.; Bujold, M. Extending ALS-Based Mapping of Forest Attributes with Medium Resolution Satellite and Environmental Data. *Remote Sens.* **2019**, *11*, 1092. [CrossRef]
79. Blázquez-Casado, Á.; Calama, R.; Valbuena, M.; Vergarechea, M.; Rodríguez, F. Combining Low-Density LiDAR and Satellite Images to Discriminate Species in Mixed Mediterranean Forest. *Ann. For. Sci.* **2019**, *76*, 57. [CrossRef]
80. Matasci, G.; Hermosilla, T.; Wulder, M.A.; White, J.C.; Coops, N.C.; Hobart, G.W.; Zald, H.S.J. Large-Area Mapping of Canadian Boreal Forest Cover, Height, Biomass and Other Structural Attributes Using Landsat Composites and Lidar Plots. *Remote Sens. Environ.* **2018**, *209*, 90–106. [CrossRef]

81. Kukkonen, M.; Maltamo, M.; Korhonen, L.; Packalen, P. Comparison of Multispectral Airborne Laser Scanning and Stereo Matching of Aerial Images as a Single Sensor Solution to Forest Inventories by Tree Species. *Remote Sens. Environ.* **2019**, *231*, 111208. [CrossRef]
82. Bolton, D.K.; Tompalski, P.; Coops, N.C.; White, J.C.; Wulder, M.A.; Hermosilla, T.; Queinnec, M.; Luther, J.E.; van Lier, O.R.; Fournier, R.A.; et al. Optimizing Landsat Time Series Length for Regional Mapping of Lidar-Derived Forest Structure. *Remote Sens. Environ.* **2020**, *239*, 111645. [CrossRef]
83. Bohlin, I.; Maltamo, M.; Hedenås, H.; Lämås, T.; Dahlgren, J.; Mehtätalo, L. Predicting Bilberry and Cowberry Yields Using Airborne Laser Scanning and Other Auxiliary Data Combined with National Forest Inventory Field Plot Data. *For. Ecol. Manag.* **2021**, *502*, 119737. [CrossRef]
84. De Almeida, D.R.A.; Broadbent, E.N.; Ferreira, M.P.; Meli, P.; Zambrano, A.M.A.; Gorgens, E.B.; Resende, A.F.; de Almeida, C.T.; do Amaral, C.H.; Corte, A.P.D.; et al. Monitoring Restored Tropical Forest Diversity and Structure through UAV-Borne Hyperspectral and Lidar Fusion. *Remote Sens. Environ.* **2021**, *264*, 112582. [CrossRef]
85. Heinaro, E.; Tanhuanpää, T.; Yrttimaa, T.; Holopainen, M.; Vastaranta, M. Airborne Laser Scanning Reveals Large Tree Trunks on Forest Floor. *For. Ecol. Manag.* **2021**, *491*, 119225. [CrossRef]
86. Baltsavias, E. Airborne Laser Scanning: Basic Relations and Formulas. *ISPRS J. Photogramm. Remote Sens.* **1999**, *54*, 199–214. [CrossRef]
87. Jakubowski, M.K.; Guo, Q.; Kelly, M. Tradeoffs between Lidar Pulse Density and Forest Measurement Accuracy. *Remote Sens. Environ.* **2013**, *130*, 245–253. [CrossRef]
88. Takahashi, T.; Awaya, Y.; Hirata, Y.; Furuya, N.; Sakai, T.; Sakai, A. Effects of Flight Altitude on Lidar-Derived Tree Heights in Mountainous. *Photogramm. J. Finl.* **2008**, *21*, 86–96.
89. Maes, J.; Teller, A.; Erhard, M.; Condé, S.; Vallecillo, S.; Barredo, J.I.; Luisa, M.; Malak, D.A.; Trombetti, M.; Vigiak, O.; et al. *Mapping and Assessment of Ecosystems and Their Services: An EU Ecosystem Assessment*; Publications Office of the EU: Luxembourg, 2020; ISBN 9789276178330.
90. Pascual, A.; De-Miguel, S. Evaluation of Mushroom Production Potential by Combining Spatial Optimization and LiDAR-Based Forest Mapping Data. *Sci. Total Environ.* **2022**, *850*, 157980. [CrossRef]
91. Bradbury, R.B.; Hill, R.A.; Mason, D.C.; Hinsley, S.A.; Wilson, J.D.; Balzter, H.; Anderson, G.Q.A.; Whittingham, M.J.; Davenport, I.J.; Bellamy, P.E. Modelling Relationships between Birds and Vegetation Structure Using Airborne LiDAR Data: A Review with Case Studies from Agricultural and Woodland Environments. *Ibis* **2005**, *147*, 443–452. [CrossRef]
92. Hill, R.A.; Hinsley, S.A.; Gaveau, D.L.A.; Bellamy, P.E. Cover: Predicting Habitat Quality for Great Tits (Parus Major) with Airborne Laser Scanning Data. *Int. J. Remote Sens.* **2004**, *25*, 4851–4855. [CrossRef]
93. Davies, A.B.; Asner, G.P. Advances in Animal Ecology from 3D-LiDAR Ecosystem Mapping. *Trends Ecol. Evol.* **2014**, *29*, 681–691. [CrossRef]
94. Simonson, W.D.; Allen, H.D.; Coomes, D.A. Applications of Airborne Lidar for the Assessment of Animal Species Diversity. *Methods Ecol. Evol.* **2014**, *5*, 719–729. [CrossRef]
95. Eid, T.; Gobakken, T.; Næsset, E. Comparing Stand Inventories for Large Areas Based on Photo-Interpretation and Laser Scanning by Means of Cost-plus-Loss Analyses. *Scand. J. For. Res.* **2004**, *19*, 512–523. [CrossRef]
96. Fassnacht, F.E.; White, J.C.; Wulder, M.A.; Næsset, E. Remote Sensing in Forestry: Current Challenges, Considerations and Directions. *For. An Int. J. For. Res.* **2024**, *97*, 11–37. [CrossRef]
97. Sparks, A.M.; Corrao, M.V.; Keefe, R.F.; Armstrong, R.; Smith, A.M.S. An Accuracy Assessment of Field and Airborne Laser Scanning–Derived Individual Tree Inventories Using Felled Tree Measurements and Log Scaling Data in a Mixed Conifer Forest. *For. Sci.* **2024**, *70*, 228–241. [CrossRef]
98. Parisi, F.; D'Amico, G.; Vangi, E.; Chirici, G.; Francini, S.; Cocozza, C.; Giannetti, F.; Londi, G.; Nocentini, S.; Borghi, C.; et al. Tree-Related Microhabitats and Multi-Taxon Biodiversity Quantification Exploiting ALS Data. *Forests* **2024**, *15*, 660. [CrossRef]
99. Ram, D.; Axelsson, A.-L.; Green, M.; Smith, H.G.; Lindström, Å. What Drives Current Population Trends in Forest Birds—Forest Quantity, Quality or Climate? A Large-Scale Analysis from Northern Europe. *For. Ecol. Manag.* **2017**, *385*, 177–188. [CrossRef]
100. Stein, A.; Gerstner, K.; Kreft, H. Environmental Heterogeneity as a Universal Driver of Species Richness across Taxa, Biomes and Spatial Scales. *Ecol. Lett.* **2014**, *17*, 866–880. [CrossRef]
101. Windrim, L.; Bryson, M. Detection, Segmentation, and Model Fitting of Individual Tree Stems from Airborne Laser Scanning of Forests Using Deep Learning. *Remote Sens.* **2020**, *12*, 1469. [CrossRef]
102. Jurjević, L.; Liang, X.; Gašparović, M.; Balenović, I. Is Field-Measured Tree Height as Reliable as Believed—Part II, A Comparison Study of Tree Height Estimates from Conventional Field Measurement and Low-Cost Close-Range Remote Sensing in a Deciduous Forest. *ISPRS J. Photogramm. Remote Sens.* **2020**, *169*, 227–241. [CrossRef]
103. Rooney, R.C.; Azeria, E.T. The Strength of Cross-taxon Congruence in Species Composition Varies with the Size of Regional Species Pools and the Intensity of Human Disturbance. *J. Biogeogr.* **2015**, *42*, 439–451. [CrossRef]

104. Balestra, M.; Marselis, S.; Sankey, T.T.; Cabo, C.; Liang, X.; Mokroš, M.; Peng, X.; Singh, A.; Stereńczak, K.; Vega, C.; et al. LiDAR Data Fusion to Improve Forest Attribute Estimates: A Review. *Curr. For. Rep.* **2024**, *10*, 281–297. [CrossRef]
105. Silva, C.; Hudak, A.; Vierling, L.; Klauberg, C.; Garcia, M.; Ferraz, A.; Keller, M.; Eitel, J.; Saatchi, S. Impacts of Airborne Lidar Pulse Density on Estimating Biomass Stocks and Changes in a Selectively Logged Tropical Forest. *Remote Sens.* **2017**, *9*, 1068. [CrossRef]
106. Hu, T.; Su, Y.; Xue, B.; Liu, J.; Zhao, X.; Fang, J.; Guo, Q. Mapping Global Forest Aboveground Biomass with Spaceborne LiDAR, Optical Imagery, and Forest Inventory Data. *Remote Sens.* **2016**, *8*, 565. [CrossRef]
107. Hansen, E.; Gobakken, T.; Næsset, E. Effects of Pulse Density on Digital Terrain Models and Canopy Metrics Using Airborne Laser Scanning in a Tropical Rainforest. *Remote Sens.* **2015**, *7*, 8453–8468. [CrossRef]
108. Wilkes, P.; Jones, S.D.; Suarez, L.; Haywood, A.; Woodgate, W.; Soto-Berelov, M.; Mellor, A.; Skidmore, A.K. Understanding the Effects of ALS Pulse Density for Metric Retrieval across Diverse Forest Types. *Photogramm. Eng. Remote Sens.* **2015**, *81*, 625–635. [CrossRef]
109. de Almeida, D.R.A.; Stark, S.C.; Shao, G.; Schietti, J.; Nelson, B.W.; Silva, C.A.; Gorgens, E.B.; Valbuena, R.; Papa, D. de A.; Brancalion, P.H.S. Optimizing the Remote Detection of Tropical Rainforest Structure with Airborne Lidar: Leaf Area Profile Sensitivity to Pulse Density and Spatial Sampling. *Remote Sens.* **2019**, *11*, 92. [CrossRef]
110. Ota, T.; Ahmed, O.; Franklin, S.; Wulder, M.; Kajisa, T.; Mizoue, N.; Yoshida, S.; Takao, G.; Hirata, Y.; Furuya, N.; et al. Estimation of Airborne Lidar-Derived Tropical Forest Canopy Height Using Landsat Time Series in Cambodia. *Remote Sens.* **2014**, *6*, 10750–10772. [CrossRef]
111. Andersen, H.-E.; Reutebuch, S.E.; McGaughey, R.J. A Rigorous Assessment of Tree Height Measurements Obtained Using Airborne Lidar and Conventional Field Methods. *Can. J. Remote Sens.* **2006**, *32*, 355–366. [CrossRef]
112. Burns, P.; Hakkenberg, C.R.; Goetz, S.J. Multi-Resolution Gridded Maps of Vegetation Structure from GEDI. *Sci. Data* **2024**, *11*, 881. [CrossRef]
113. Su, H.; Shen, W.; Wang, J.; Ali, A.; Li, M. Machine Learning and Geostatistical Approaches for Estimating Aboveground Biomass in Chinese Subtropical Forests. *For. Ecosyst.* **2020**, *7*, 64. [CrossRef]
114. Sun, C.; Cao, S.; Sanchez-Azofeifa, G.A. Mapping Tropical Dry Forest Age Using Airborne Waveform LiDAR and Hyperspectral Metrics. *Int. J. Appl. Earth Obs. Geoinf.* **2019**, *83*, 101908. [CrossRef]
115. de Almeida, C.T.; Galvão, L.S.; de Oliveira Cruz e Aragão, L.E.; Ometto, J.P.H.B.; Jacon, A.D.; de Souza Pereira, F.R.; Sato, L.Y.; Lopes, A.P.-T.; de Alencastro Graça, P.M.L.; de Jesus Silva, C.V.; et al. Combining LiDAR and Hyperspectral Data for Aboveground Biomass Modeling in the Brazilian Amazon Using Different Regression Algorithms. *Remote Sens. Environ.* **2019**, *232*, 111323. [CrossRef]
116. Fayad, I.; Baghdadi, N.; Lahssini, K. An Assessment of the GEDI Lasers' Capabilities in Detecting Canopy Tops and Their Penetration in a Densely Vegetated, Tropical Area. *Remote Sens.* **2022**, *14*, 2969. [CrossRef]
117. Su, Y.; Wu, Z.; Zheng, X.; Qiu, Y.; Ma, Z.; Ren, Y.; Bai, Y. Harmonizing Remote Sensing and Ground Data for Forest Aboveground Biomass Estimation. *Ecol. Inform.* **2025**, *86*, 103002. [CrossRef]
118. Francini, S.; Vangi, E.; D'Amico, G.; Borghi, C.; Cencini, G.; Monari, C.; Zolli, C.; Chirici, G. Field-Independent Carbon Mapping and Quantification in Forest Plantation through Remote Sensing. *Eur. J. Remote Sens.* **2024**, *57*, 2334717. [CrossRef]
119. Chave, J.; Davies, S.J.; Phillips, O.L.; Lewis, S.L.; Sist, P.; Schepaschenko, D.; Armston, J.; Baker, T.R.; Coomes, D.; Disney, M.; et al. Ground Data Are Essential for Biomass Remote Sensing Missions. *Surv. Geophys.* **2019**, *40*, 863–880. [CrossRef]
120. Duncanson, L.; Kellner, J.R.; Armston, J.; Dubayah, R.; Minor, D.M.; Hancock, S.; Healey, S.P.; Patterson, P.L.; Saarela, S.; Marselis, S.; et al. Aboveground Biomass Density Models for NASA's Global Ecosystem Dynamics Investigation (GEDI) Lidar Mission. *Remote Sens. Environ.* **2022**, *270*, 112845. [CrossRef]
121. Martino, A.J.; Neumann, T.A.; Kurtz, N.T.; McLennan, D. ICESat-2 Mission Overview and Early Performance. In Proceedings of the Sensors, Systems, and Next-Generation Satellites XXIII, Strasbourg, France, 9–12 September 2019; Neeck, S.P., Kimura, T., Martimort, P., Eds.; SPIE: Bellingham, WA, USA, 2019; p. 11.
122. Nilsson, M.; Nordkvist, K.; Jonzén, J.; Lindgren, N.; Axensten, P.; Wallerman, J.; Egberth, M.; Larsson, S.; Nilsson, L.; Eriksson, J.; et al. A Nationwide Forest Attribute Map of Sweden Predicted Using Airborne Laser Scanning Data and Field Data from the National Forest Inventory. *Remote Sens. Environ.* **2017**, *194*, 447–454. [CrossRef]
123. Valbuena, R.; Maltamo, M.; Packalen, P. Classification of Forest Development Stages from National Low-Density Lidar Datasets: A Comparison of Machine Learning Methods. *Rev. Teledetección* **2016**, *45*, 15–25. [CrossRef]
124. Liang, M.; Duncanson, L.; Silva, J.A.; Sedano, F. Quantifying Aboveground Biomass Dynamics from Charcoal Degradation in Mozambique Using GEDI Lidar and Landsat. *Remote Sens. Environ.* **2023**, *284*, 113367. [CrossRef]
125. Fareed, N.; Numata, I. Evaluating the Impact of Field-Measured Tree Height Errors Correction on Aboveground Biomass Modeling Using Airborne Laser Scanning and GEDI Datasets in Brazilian Amazonia. *Trees For. People* **2025**, *19*, 100751. [CrossRef]
126. Gobakken, T.; Næsset, E. Estimation of Diameter and Basal Area Distributions in Coniferous Forest by Means of Airborne Laser Scanner Data. *Scand. J. For. Res.* **2004**, *19*, 529–542. [CrossRef]

127. Naesset, E.; Okland, T.; Næsset, E.; Økland, T. Estimating Tree Height and Tree Crown Properties Using Airborne Scanning Laser in a Boreal Nature Reserve. *Remote Sens. Environ.* **2002**, *79*, 105–115. [CrossRef]
128. Lefsky, M.A.; Cohen, W.B.; Harding, D.J.; Parker, G.G.; Acker, S.A.; Gower, S.T. Lidar Remote Sensing of Above-ground Biomass in Three Biomes. *Glob. Ecol. Biogeogr.* **2002**, *11*, 393–399. [CrossRef]
129. Lefsky, M.A.; Harding, D.J.; Keller, M.; Cohen, W.B.; Carabajal, C.C.; Del Bom Espirito-Santo, F.; Hunter, M.O.; de Oliveira, R. Estimates of Forest Canopy Height and Aboveground Biomass Using ICESat. *Geophys. Res. Lett.* **2005**, *32*, L22S02. [CrossRef]
130. Patenaude, G.; Hill, R.; Milne, R.; Gaveau, D.L.A.; Briggs, B.B.J.; Dawson, T.P. Quantifying Forest above Ground Carbon Content Using LiDAR Remote Sensing. *Remote Sens. Environ.* **2004**, *93*, 368–380. [CrossRef]